NASA TECHNICAL NOTE

NASA TN D-3093

NASA TN D-3093

DISTRIBUTION STATEMENT A
Approved for public release
Distribution Unlimited

19960628 079

PERFORMANCE OF FIVE ABLATION MATERIALS AS COATINGS FOR STRUCTURES IN A REGION OF SEPARATED FLOW

by Louis E. Clark and Allen G. McLain

Langley Research Center
Langley Station, Hampton, Va.

DTIC QUALITY INSPECTED 1

NATIONAL AERONAUTICS AND SPACE ADMINISTRATION - WASHINGTON, D. C. - NOVEMBER

DEPARTMENT OF DEFENSE
PLASTICS TECHNICAL EVALUATION CENTER
PICATINNY ARSENAL, DOVER, N. J.

AQ8

DISCLAIMER NOTICE

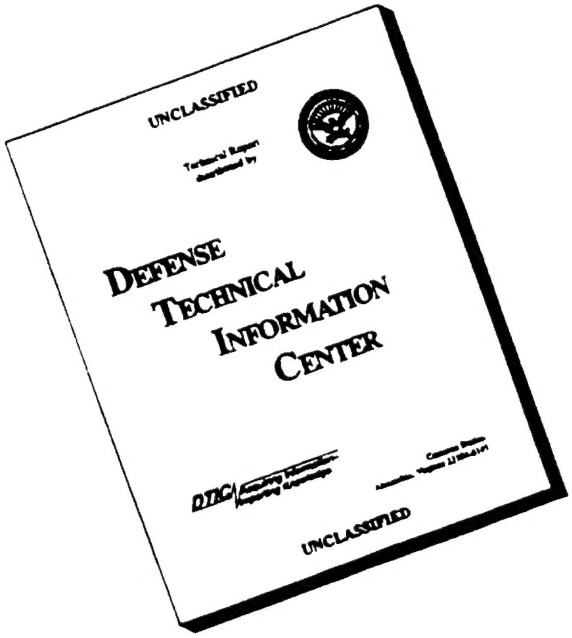

THIS DOCUMENT IS BEST QUALITY AVAILABLE. THE COPY FURNISHED TO DTIC CONTAINED A SIGNIFICANT NUMBER OF PAGES WHICH DO NOT REPRODUCE LEGIBLY.

NASA TN D-3093

PERFORMANCE OF FIVE ABLATION MATERIALS AS COATINGS FOR STRUCTURES IN A REGION OF SEPARATED FLOW

By Louis E. Clark and Allen G. McLain

Langley Research Center
Langley Station, Hampton, Va.

NATIONAL AERONAUTICS AND SPACE ADMINISTRATION

For sale by the Clearinghouse for Federal Scientific and Technical Information
Springfield, Virginia 22151 – Price $2.00

PERFORMANCE OF FIVE ABLATION MATERIALS AS COATINGS FOR STRUCTURES IN A REGION OF SEPARATED FLOW

By Louis E. Clark and Allen G. McLain
Langley Research Center

SUMMARY

An investigation was made of several commercially available ablation materials for use as thermal protection for the sidewalls of advanced air-to-air missiles. Material specimens of different thickness were tested on the cylindrical section of a rounded-ogive-cylinder model. The tests were conducted in the Langley 11-inch ceramic-heated tunnel at a heating rate, enthalpy, and free-stream Mach number typical of the values of these parameters encountered during a missile trajectory. Oil-flow and pressure tests showed that the boundary layer had separated from the cylindrical section of the model and that the entire specimen region was immersed in separated flow. In the separated-flow environment, a phenolic-cork composition was found to be superior to the other materials studied in limiting the substrate temperature rise. The phenolic-cork composition experienced considerably greater erosion than the phenolic-nylon, asbestos-phenolic, and subliming-salt compositions, which ranked second, third, and fourth, respectively, in limiting the substrate temperature rise; however, these materials developed either surface cracks or large fissures in the char layer. Preconditioning of the phenolic-cork, asbestos-phenolic, and epoxy-solid materials by heat cycling to 400° F (478° K) did not decrease their thermal performance.

INTRODUCTION

It is anticipated that air-to-air missiles, which will be employed by advanced supersonic fighter aircraft, will fly at velocities high enough to require thermal protection on the sidewalls as well as in the stagnation regions. During a typical trajectory, the missile sidewalls may experience heating rates up to about 15 Btu/ft^2-sec (170 kW/m^2) with radiation equilibrium temperatures of 1500° F (1089° K). The use of heat-resistant metals to provide the required thermal protection would impose a large weight penalty. A promising approach to provide a lightweight thermal-protection system for the sidewalls of such missiles is the use of a low-density ablating material applied to an aluminum substructure. Therefore, a limited test program has been conducted to evaluate several ablation materials on the basis of the weight required to limit the substructure to a given temperature rise, the amount of material eroded, and the char-layer characteristics.

The investigation was conducted in the Langley 11-inch ceramic-heated tunnel at a heating rate of 10 Btu/ft^2-sec (113 kW/m^2), at an enthalpy of 900 Btu/lb (2.09 MJ/kg), and at a free-stream Mach number of 6, which are typical values for these parameters experienced by the missile sidewalls during a trajectory. The material specimens were mounted on the cylindrical section of a rounded-ogive-cylinder model to obtain the desired heating rate. Four materials were selected for evaluation on the basis of their insulative characteristics, ease of application, and commercial availability. The four materials selected were: (a) a phenolic-cork composition, (b) an asbestos tape-phenolic composition, (c) a two-part epoxy and solid composition, and (d) a composition of an inorganic subliming salt and an organic binder. The first two materials may be wrapped or molded to shape and bonded to the substructure while the latter two are sprayed directly to the substructure. In addition, a low-density molded phenolic-nylon-silica composition formulated at NASA Langley Research Center was tested. This report presents the results of the test program.

SYMBOLS

The units used in the present paper are given in both U.S. Customary Units and the International System of Units (SI). Factors relating the two systems are given in reference 1.

c_p	specific heat of calorimeter material, Btu/lb-$^\circ$R (J/kg $^\circ$K)
E	thermal effectiveness, Btu/lb (J/kg)
L	distance from flow separation point to rear of specimen, in. (cm)
q_c	cold-wall heating rate, Btu/ft^2-sec (W/m^2)
t	time, sec
T_w	temperature of calorimeter wall, $^\circ$F ($^\circ$K)
ΔT	substructure temperature rise at back surface, $^\circ$F ($^\circ$K)
W	weight of protection material per unit area, lb/ft^2 (kg/m^2)
x	distance from separation point, in. (cm)
τ	thickness of calorimeter wall, ft (cm)
ρ	density of calorimeter material, lb/ft^3 (kg/m^3)

APPARATUS AND TESTS

Langley 11-Inch Ceramic-Heated Tunnel

The materials were tested in the Langley 11-inch ceramic-heated tunnel (fig. 1) which is equipped with a Mach 6 nozzle. This facility consists of a large cylindrical pressure vessel lined with refractory brick and filled with zirconia and alumina spheres. The spheres are heated by the products of combustion from a gas burner until the desired bed temperature is reached. The burner is then turned off and air is brought in at the bottom of the vessel and is heated by passing through the bed. After being heated by the bed, the air expands through a conical nozzle and flows through the free-jet test section and diffuser to the atmosphere. When the desired conditions have been established, the model is inserted into the test section from the model bay by means of a model-insertion mechanism. A photograph of the model inserted in the test section is shown in figure 2. The tunnel is described in detail in references 2 and 3.

Test Model

In order to obtain the desired heating rate, the material specimens were mounted on the cylindrical section of a rounded-ogive-cylinder model. The model, shown in figure 3, had four rectangular cavities or blanks in the cylindrical section in which the material specimens were mounted. Errors due to conduction of heat from the specimen to the model body were minimized by restricting the conduction paths by the use of screws to hold and support the specimen. The model was constructed of copper and had a total length of $8\frac{3}{8}$ inches (21.27 cm) and a diameter of $3\frac{3}{4}$ inches (9.53 cm). The nose shape was a rounded-tangent-ogive configuration with a ring installed on the nose as a boundary-layer trip. The model was water cooled to prevent excessive heating of the nose and thermocouple leads.

Heat-Transfer Models

The cold-wall heat flux to the material test region was determined by using two different calorimeters which were designed to fit in the model test blanks. The two calorimeters used were a thin-wall slope type of calorimeter and a commercial continuous-reading type of calorimeter. The continuous-reading calorimeter gives the variation of heating rate with time, whereas the slope calorimeter gives the heating rate at only one time for each insertion in the test stream. However, the slope calorimeter is much simpler to construct and use.

Thin-wall slope type of calorimeter.- The thin-wall slope type of calorimeter is illustrated in figure 4(a). It consists of a thin wall contoured to the model shape with thermocouples attached to the back surface. The calorimeter is constructed with a thin wall to minimize conduction errors. With the

calorimeter installed in the test blank on the afterbody, the model is rapidly inserted into the stream and the change of wall temperature with time is recorded by an oscillograph. The change of wall temperature with time was measured 0.1 second after the model reached the stream center line. At this time, transient effects were not present and it is believed that conduction along the surface was negligible since the calorimeter was still essentially isothermal. The time rate of change of the wall temperature and the wall material properties are substituted in the following equation to obtain the heating rate:

$$q_c = \rho \tau c_p \frac{dT_w}{dt}$$

Continuous-reading calorimeter.- The continuous-reading calorimeter consists of a thin disk which is fastened along its edge to a heat sink. The application of a heat flux to the disk causes a flow of heat from the center of the disk to its edge. One wire of a thermocouple pair is attached to the center back surface of the disk and forms a hot junction; the other thermocouple wire is attached to the heat sink at the edge of the disk to form the cold junction of a differential thermocouple. The output of the thermocouple pair, which measures the temperature drop between the disk center and edge, is proportional to the heating rate. Calibration curves for the calorimeter were supplied by the manufacturer and an analysis of this type of calorimeter is given in reference 4. Figure 4(b) is a section view of the calorimeter fitted into a mounting plate which is installed in a blank on the model cylindrical section.

Pressure-Distribution Model

Model static pressures in the material testing regions were measured with the orifice plate shown in figure 5 which was installed in the model blanks. The plate was contoured to the body shape and contained orifices at the same streamwise locations as those at which heat-transfer measurements were made; an additional orifice was located at the rear of the specimen region. The orifices were 0.03 inch (0.076 cm) in diameter and monel and plastic tubing connected the orifice to a strain-gage pressure transducer.

Ablation-Material Specimens

The material test specimens consisted of varying thicknesses of the materials bonded to a 0.05-inch-thick (0.127-cm) aluminum substrate to which thermocouples were attached. The arrangement is shown in figure 6. The specimens were 3 inches (7.62 cm) long and 1 inch (2.54 cm) wide and were made to fit snugly in the blanks on the model cylindrical section. The materials were bonded to the aluminum substrate by means of an epoxy adhesive, which was used because of its ability to form a strong bond with aluminum. Specimens of 0.10, 0.20, and 0.25 inch (0.254, 0.508, and 0.635 cm) thickness were tested.

The materials tested in this investigation are enumerated in table I. The density of these materials ranges from 30 to 62 lb/ft^3 (480.6 to 993.2 kg/m^3). All the materials, with the possible exception of the subliming salt, were expected to form chars during ablation. Each of the five materials is available commercially and all have relatively low thermal conductivities.

To investigate the effect of the prelaunch heating which occurs when missiles are carried externally by high-performance aircraft, several of the materials were heat cycled from -65° F to 400° F (219° K to 478° K) before testing. This cycling simulates a number of aircraft flights under a wide range of local climatic conditions. During the heat cycling, the materials were held at 400° F (478° K) for a total of 50 minutes to simulate the heating occurring at the aircraft top speed.

Test Procedure and Tunnel Conditions

The procedure followed for testing consisted of: (1) Establishing tunnel conditions (stagnation temperature of 2800° F (1810° K) and stagnation pressure of 1015 psia (7.0 MN/m^2)), (2) allowing equilibrium to be reached, and (3) exposing the model, with specimens in place, to the flow for 60 seconds.

During the exposure to the flow, the surface behavior of each material was observed on high-speed motion-picture film, and, in some tests, shadowgraph pictures were taken. Thermocouple and pressure-transducer outputs were monitored with oscillograph recorders. The tunnel operating conditions are summarized in table II, and the measurement of the tunnel stagnation temperature and Mach number is discussed in references 2 and 3.

To define the flow in the specimen region, a series of tests was conducted with the calorimeter and pressure-orifice plates installed in the blanks on the model cylindrical section. To avoid possible interference effects, the model was oriented so that three of the test blanks were located out of the proximity of the support strut, and these blanks were used to test the material specimens.

RESULTS AND DISCUSSION

Determination of Test Environment

The streamwise heat-flux distribution measured at the three specimen test locations on the model cylindrical section is shown in figure 7. The heat flux over the test locations was found to increase in the streamwise direction by about 35 percent, and up to about 20-percent differences in heating rate existed between the three test positions at the same longitudinal location. As shown in figure 7, the heating rate increased from approximately double the calculated laminar value (ref. 5) near the front of the specimens and reached values approximately equal to the calculated turbulent heating rates in the material test region. In view of this variation, further tests and analysis were made to define the test flow conditions.

Streamwise measurements of model static pressure gave a constant value of 1.75 psia (12.1 kN/m^2) over the length of the specimen region whereas a static pressure of about 0.9 psia (6.2 kN/m^2) would normally be expected in this region. The abnormally high static pressure and increasing streamwise heating rate were suggestive of possible boundary-layer separation, and, to explore this possibility, a series of oil-drop tests were made in which the movement of droplets of an oil and soot mixture over the surface of the model was photographed during a test. Figure 8, which is a typical oil-drop photograph, shows that reverse flow characteristic of a separated boundary layer was occurring over the model cylindrical section, and that the test positions were completely immersed in separated flow. The separation point is indicated by the ring of oil which is located near the nose cylinder junction of the model. This ring is formed by the oil flowing back over the nose merging with the forward flow of oil from the separated region. No evidence of reattachment of the boundary layer on the model was observed.

The state of the separated boundary layer was not definitely determined from these tests, although it is probably transitional or turbulent. Shadowgraph studies showed the presence of a shock at the separation point, but the shadowgraph was not sensitive enough to bring out the details of the boundary layer in the separated region. To investigate the state of the separated boundary layer further, the heating-rate distributions were compared with the distributions for cavity and large-scale wedge types of separation reported in the literature. However, these distributions were considerably different from those of the present tests. References 6, 7, and 8 report that the heat flux for the laminar and turbulent separated boundary layers for cavity and large-scale wedge types of separation decreased below the attached boundary-layer value near the separation point and remained at about 56 percent of the attached value until the reattachment point was approached, at which point, the heat flux increased rapidly. In the present tests (as shown in fig. 7) the heat flux was considerably above the attached laminar value a short distance downstream of separation and increased rapidly to the turbulent value although the boundary layer apparently did not reattach on the model. In addition to attached flow, regions of separated flow may exist on air-to-air missiles and, therefore, tests were conducted to determine the behavior of ablation materials under separated-flow conditions.

Material Evaluation

The materials were evaluated on the basis of the weight required to limit the substrate temperature rise to a given value, the amount of material eroded, and the char characteristics.

Substrate temperature rise.- A limit of 100° F (56° K) in substrate temperature rise was selected because missiles carried externally by high-performance aircraft may experience temperatures up to 350° F (450° K) due to aerodynamic heating caused by the velocity of the aircraft. An increase of 100° F (56° K) during the missile flight gives a final substrate temperature of 450° F (506° K), which was taken as the design temperature limit for an aluminum substructure because of the decrease in strength of aluminum alloys at

elevated temperatures. It was considered desirable to evaluate the materials at a common heating rate, and, since the heat flux to the specimen varied not only with distance along the specimen but also with the test position as shown in figure 7, the materials were evaluated at the streamwise location for each position which corresponded to a heating rate of 10 Btu/ft^2-sec (113 kW/m^2).

To evaluate the materials, a plot of the total heat input required for a 100° F (56° K) rise in substrate temperature against the material weight per unit area was made, as shown in figure 9. From this figure it is evident that the material represented by the line with the greatest slope exhibits the superior performance. The phenolic-cork performs best in protecting the substrate from a 100° F (56° K) temperature rise at all weights per unit area tested. The asbestos-phenolic, subliming-salt, and phenolic-nylon compositions fall considerably below phenolic-cork. The asbestos-phenolic and phenolic-nylon have about the same performance whereas the subliming salt is somewhat lower. The epoxy solid is seen to have the lowest performance of the five materials tested.

Figure 10 shows the results of tests of heat-cycled specimens of the phenolic-cork, asbestos-phenolic, and epoxy-solid compositions. It can be seen that heat cycling did not significantly decrease the insulation performance of these materials.

Char characteristics.- Although the phenolic-cork composition was superior to the other materials tested from an insulation standpoint, it experienced more erosion than did phenolic-nylon, the subliming-salt, or the asbestos-phenolic compositions. Based on erosion alone, any of these materials would be more suitable than phenolic-cork. The epoxy-solid composition not only had the lowest insulation performance but also experienced the greatest erosion of the materials tested. The relative erosion of the materials can be seen in the photographs of the sectioned specimens in figure 11. The lightly shaded area shows the specimen shape before testing while the darker area is a photograph of the specimen after testing. Also apparent is the greater erosion which occurred at the rear portion of the specimens where the highest heating rate was experienced.

The erosion of the materials was probably strongly influenced by the char character. Phenolic-cork formed a soft, powdery char which is easily sheared from the virgin material. Photographs of the phenolic-cork before and after testing are shown in figure 12(a). The phenolic-nylon, the subliming-salt, and the asbestos-phenolic compositions experienced very little erosion and all formed a relatively thick char zone. The phenolic-nylon developed deep fissures in the char which could have reduced its insulating performance. These fissures are visible in figure 12(b). The phenolic-nylon char was very hard and was probably strengthened by melted silicon dioxide formed from the silica Ecco-spheres. The subliming salt also developed fissures in the surface as shown in figure 12(c). These cracks were not as deep nor as extensive as those formed in phenolic-nylon and appeared to emanate from local blisters in the surface. Most of the blisters were observed at the rear of the specimens where the highest heating rate was experienced. A very small change of shape occurred for the asbestos-phenolic composition; however, as can be seen in figure 12(d),

this material also developed surface cracks. The cracks were relatively deep and were caused by separation between layers of the molding tape which was wrapped at an angle of 30° to the aluminum substrate in fabricating the specimens. The epoxy-solid formed a thin char layer which spalled in flakes sometimes approximately 0.5 inch (1.27 cm) in diameter. The char was very hard and porous. Photographs of the epoxy-solid before and after testing are shown in figure 12(e).

In summary, the phenolic-nylon, asbestos-phenolic, and subliming-salt compositions which ranked second, third, and fourth, respectively, in insulation performance, looked better from an erosion standpoint; however, these three materials developed surface cracks or large fissures in the char surface. The phenolic-cork and epoxy-solid compositions exhibited large surface erosion rates, which could be an important factor in applications where large shape changes would affect the aerodynamic characteristics of the missile.

Thermal Effectiveness

The product of the cold-wall heating rate and the time for a given substrate temperature rise divided by the weight of protection material per unit area $E = \frac{q_c t}{W}$ is frequently used as a measure of the thermal effectiveness of charring ablation materials. This parameter is referred to in the literature by a number of names including: insulation efficiency, thermal effectiveness, thermal shielding efficiency, and effective heat capacity.

The variation of thermal effectiveness (based on a 100° F (56° K) substrate temperature rise) with heat shield weight per unit area is shown in figure 13. It is seen that the phenolic-cork maintains a constant effectiveness as the unit weight is increased by a factor of $2\frac{1}{2}$ whereas the phenolic-nylon, subliming-salt, epoxy-solid, and asbestos-phenolic compositions show increases of 15 percent to 30 percent initially, and then as the unit weight is increased over two times, the thermal effectiveness appears to approach a constant value.

For the single thickness of 0.1 inch (0.254 cm), a substrate temperature rise of 300° F (167° K) was attained for each material except cork, which required an extrapolation of 100° F (56° K). Figure 14 shows the thermal effectiveness as a function of substrate temperature rise for the 0.1-inch-thick (0.254-cm) specimens. An increase of a factor of 3 in the allowable substrate temperature rise (from 100° F (56° K) to 300° F (167° K)) resulted in an increase in thermal effectiveness of about a factor of 2 for all materials. Phenolic-cork maintained about the same relative superior performance over the range of substrate temperatures with the exception of phenolic-nylon. The thermal effectiveness of phenolic-nylon increased at a greater rate with substrate temperature rise than phenolic-cork, and consequently the relative superiority of phenolic-cork over phenolic-nylon decreased at the higher temperatures.

An estimate of the effect of the separated boundary layer on the material performance can be obtained by a comparison of the phenolic-cork data of the present tests with data from tests reported in reference 9. This reference reports tests of 0.10-inch-thick (0.254-cm) phenolic-cork at comparable heating rates but at enthalpies from 4000 to 8000 Btu/lb (9.3 to 18.6 MJ/kg) as compared with 900 Btu/lb (2.09 MJ/kg) of the present tests. However, no effect of enthalpy on thermal effectiveness was detected over the range from 4000 to 8000 Btu/lb (9.3 to 18.6 MJ/kg). In addition, reference 9 cites data from tests at much lower enthalpies which appear to agree with their data and therefore concludes that enthalpy played only a secondary role in influencing the behavior of high-temperature charring-composite materials. The phenolic-cork data from the present tests are shown in figure 15 compared with the data from reference 9. Data from reference 9 for tests conducted in both air and nitrogen are shown in figure 15. The data for tests in nitrogen have been included as a guide to the trend of the limited data for tests in air. The thermal effectiveness in the separated boundary layer is seen to be about 30 percent higher than the effectiveness obtained in an attached laminar boundary layer in air. Although differences in substrate heat capacity and bonding agent existed between the tests, data reported in reference 9 indicate that these differences probably would not cause changes in thermal effectiveness exceeding 10 percent. Therefore, it is concluded that the performance of the phenolic-cork in the separated boundary layer is not grossly different from its performance in an attached laminar boundary layer.

CONCLUDING REMARKS

Several commercially available charring ablators have been experimentally evaluated in a separated boundary layer at a heating rate of approximately 10 Btu/ft^2-sec (113 kW/m^2) and at an enthalpy of 900 Btu/lb (2.09 MJ/kg). The tests were conducted in a ceramic-heated airstream at a free-stream Mach number of 6.

A phenolic-cork composition was found to be superior to the other materials tested on the basis of the weight required to insulate the substrate against a 100° F (56° K) rise in temperature. Thermal preconditioning of the phenolic-cork composition did not alter its insulation performance.

The phenolic-cork experienced considerably greater erosion than the phenolic-nylon, asbestos-phenolic, and the subliming-salt compositions which ranked second, third, and fourth, respectively, in limiting the substrate temperature rise; however, these materials developed either surface cracks or large fissures in the char layer.

The thermal effectiveness of the phenolic-cork composition in the separated boundary layer was not grossly different from the effectiveness reported by NASA Technical Note D-1889 in an attached laminar boundary layer at the same heating rate, but at a considerably higher enthalpy.

Increasing the heat-shield weight by a factor of $2\frac{1}{2}$ resulted in no change in the thermal effectiveness for the phenolic-cork composition while the asbestos-phenolic, epoxy-solid, phenolic-nylon, and subliming-salt compositions showed initial increases in effectiveness of 15 to 20 percent and then tended to approach a constant effectiveness as the heat-shield weight was increased over two times.

Langley Research Center,
National Aeronautics and Space Administration,
Langley Station, Hampton, Va., August 20, 1965.

REFERENCES

1. Mechtly, E. A.: The International System of Units - Physical Constants and Conversion Factors. NASA SP-7012, 1964.

2. Trout, Otto F., Jr.: Design, Operation, and Testing Capabilities of the Langley 11-Inch Ceramic-Heated Tunnel. NASA TN D-1598, 1963.

3. Midden, Raymond E.; and Cocke, Bennie W., Jr.: Diffuser Performance of a Mach 6 Open-Jet Tunnel and Model-Blockage Effects at Stagnation Temperatures to 3,600° F. NASA TN D-2384, 1964.

4. Gardon, Robert: An Instrument for the Direct Measurement of Intense Thermal Radiation. Rev. Sci. Instr., vol. 24, no. 5, May 1953, pp. 366-370.

5. Harms, Richard J.; Schmidt, Craig M.; Hanawalt, Arnold J.; and Schmitt, Durwin A.: A Manual for Determining Aerodynamic Heating of High-Speed Aircraft - Volume I. Rept. No. 7006-3352-001, Bell Aircraft Corp., June 1959.

6. Larson, Howard K.: Heat Transfer in Separated Flows. J. Aero/Space Sci., vol. 26, no. 11, Nov. 1959, pp. 731-738.

7. Schaefer, John W.; and Ferguson, Harold: Investigation of Separation and Associated Heat Transfer and Pressure Distribution on Cone-Cylinder-Flare Configurations at Mach Five. ARS J., vol. 32, no. 5, May 1962, pp. 762-769.

8. Bogdonoff, S. M.; and Vas, I. E.: Some Experiments on Hypersonic Separated Flows. ARS J., vol. 32, no. 10, Oct. 1962, pp. 1564-1572.

9. Vojvodich, Nick S.; and Winkler, Ernest L.: The Influence of Heating Rate and Test Stream Oxygen Content on the Insulation Efficiency of Charring Materials. NASA TN D-1889, 1963.

TABLE I.- MATERIAL DESIGNATION, DENSITY, AND DESCRIPTION

Material	Density		Description
	lb/ft^3	kg/m^3	
Phenolic-cork composition	30.0	480.6	80% natural cork 20% phenolic-binder Applied by wrapping
Asbestos-phenolic composition	32.0	512.6	Asbestos paper with organic filler and phenolic-resin binder Tape form
Subliming salt composition	62.0	993.2	Inorganic salt with organic binder Spray applied
Epoxy-solid composition	50.0	801.0	Two-part epoxy base with high solid content Spray applied
Phenolic-nylon (PN-4)	36.0	576.7	15.8% phenolic-resin 15.8% phenolic Microballoons 5.0% silica Eccospheres 63.4% nylon Molded

TABLE II.- TUNNEL OPERATING CONDITIONS

Stagnation pressure, psia (MN/m^2)	1015	(7.0)
Stagnation temperature, ^{o}F (^{o}K)	2800	(1810)
Enthalpy, Btu/lb (MJ/kg)	900	(2.09)
Free-stream Mach number	6.1	
Free-stream static pressure, psia (kN/m^2)	0.53	(3.65)
Free-stream velocity, ft/sec (m/sec)	6700	(2042)
Run time, sec	60	

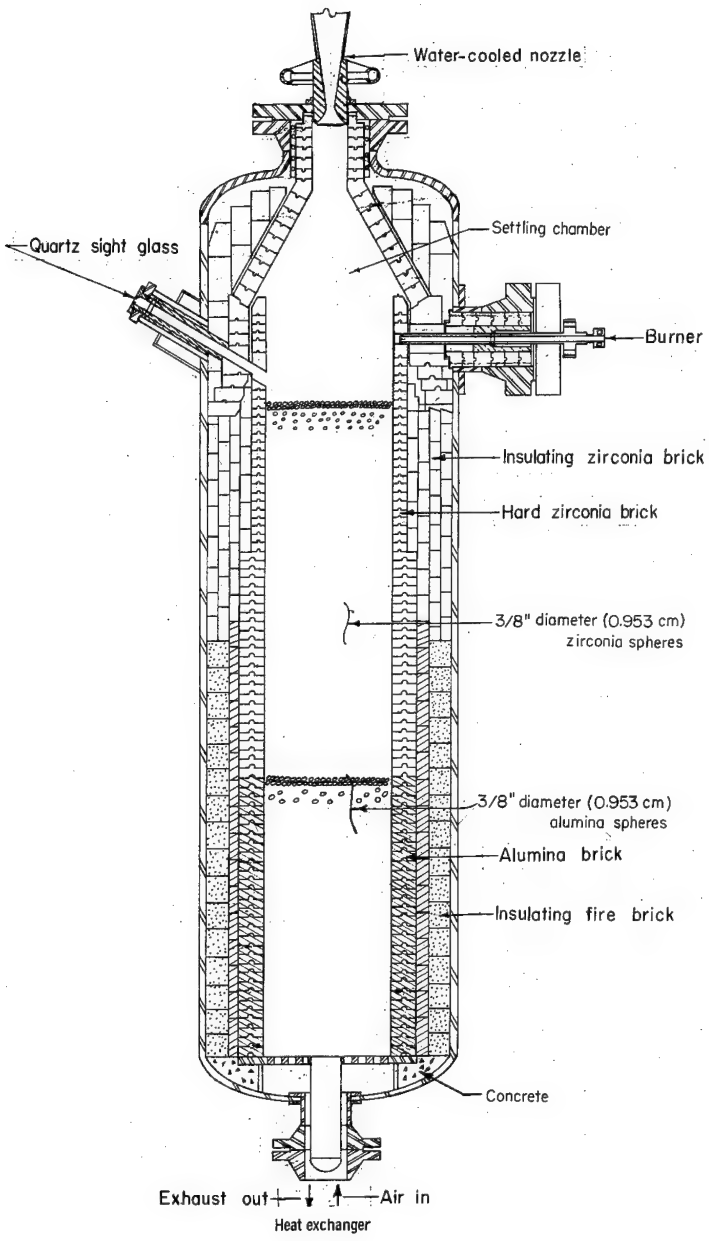

(a) Heat exchanger.

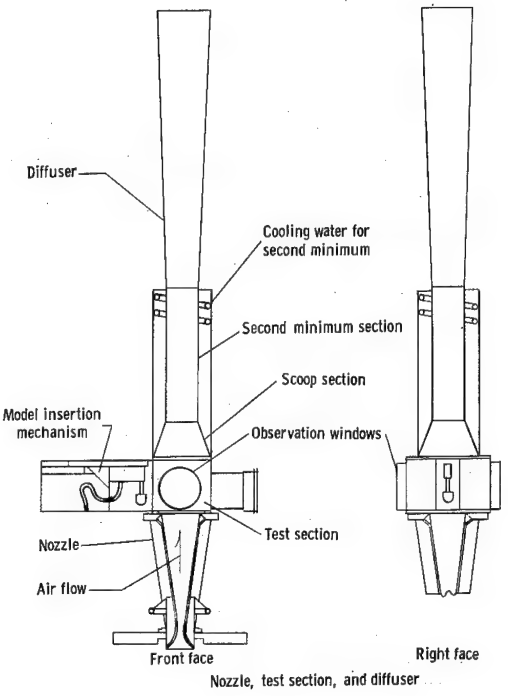

(b) Nozzle, test section, and diffuser.

Figure 1.- Components of Langley 11-inch ceramic-heated tunnel.

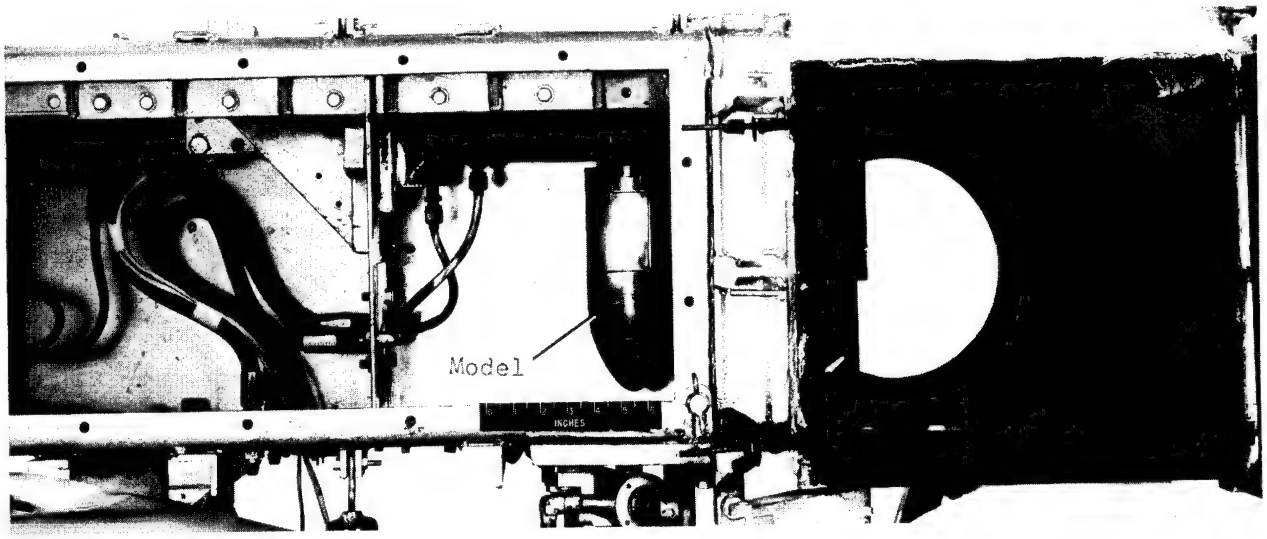

(a) Model retracted. L-65-2688.1

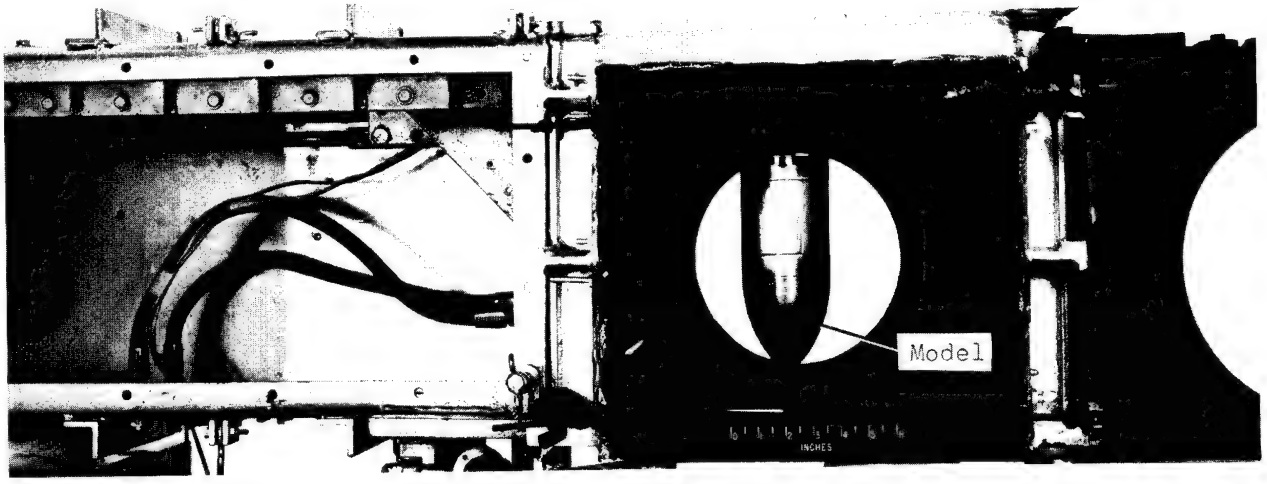

(b) Model in airstream. L-65-2687.1

Figure 2.- Photographs of model retracted and model in airstream.

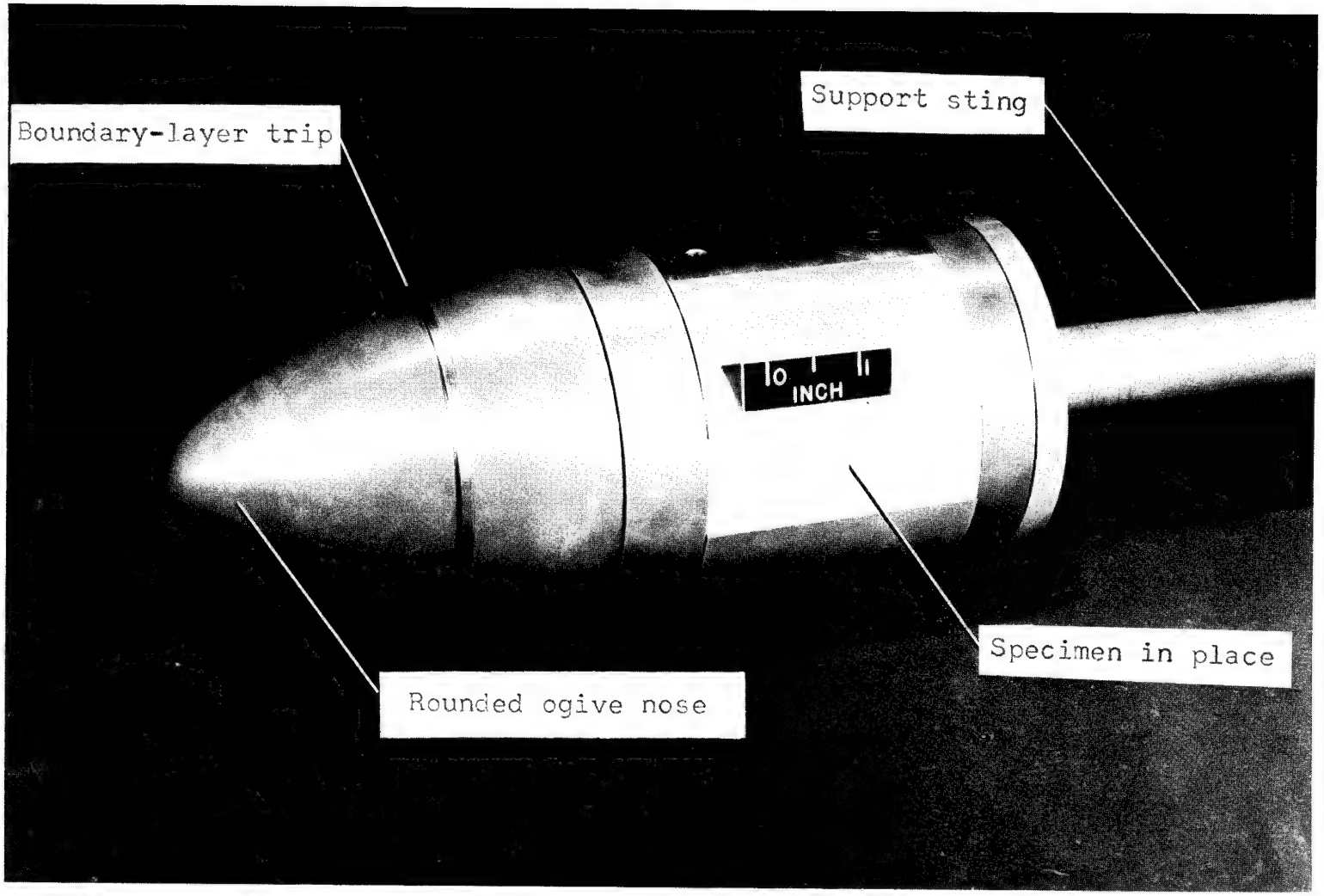

(a) Model assembled for testing.

L-63-7022.1

Figure 3.- Model for specimen support.

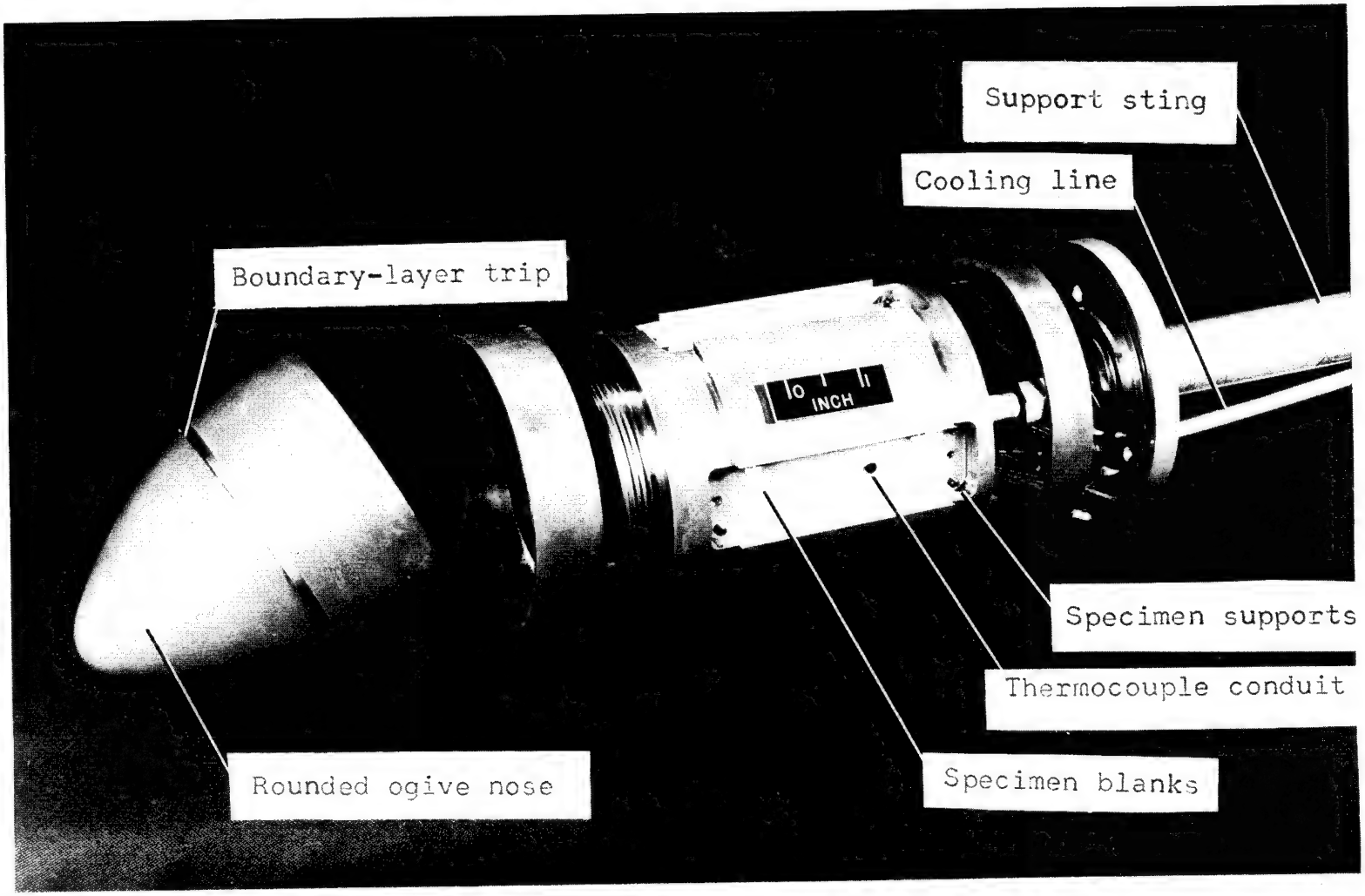

(b) Model disassembled.

L-63-7045.1

Figure 3.- Concluded.

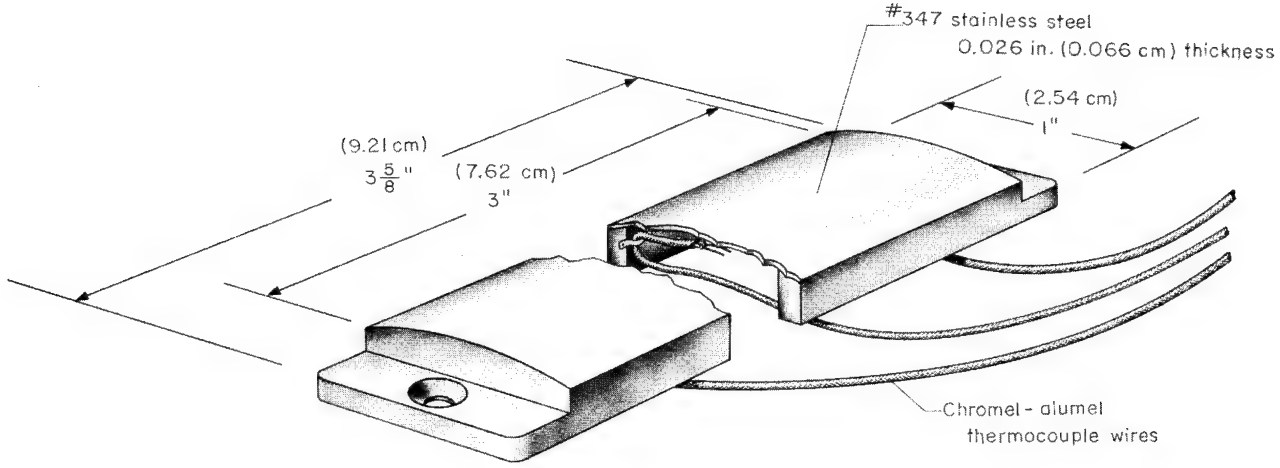

(a) Thin-wall slope calorimeter.

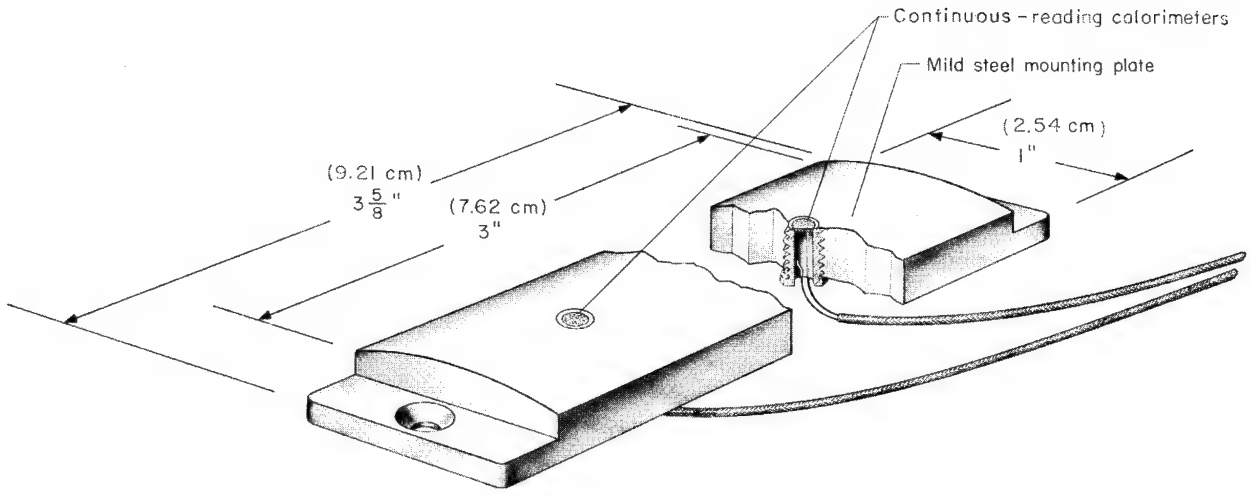

(b) Mounting plate for two continuous-reading calorimeters.

Figure 4.- Calorimeters used to determine heat flux in specimen region.

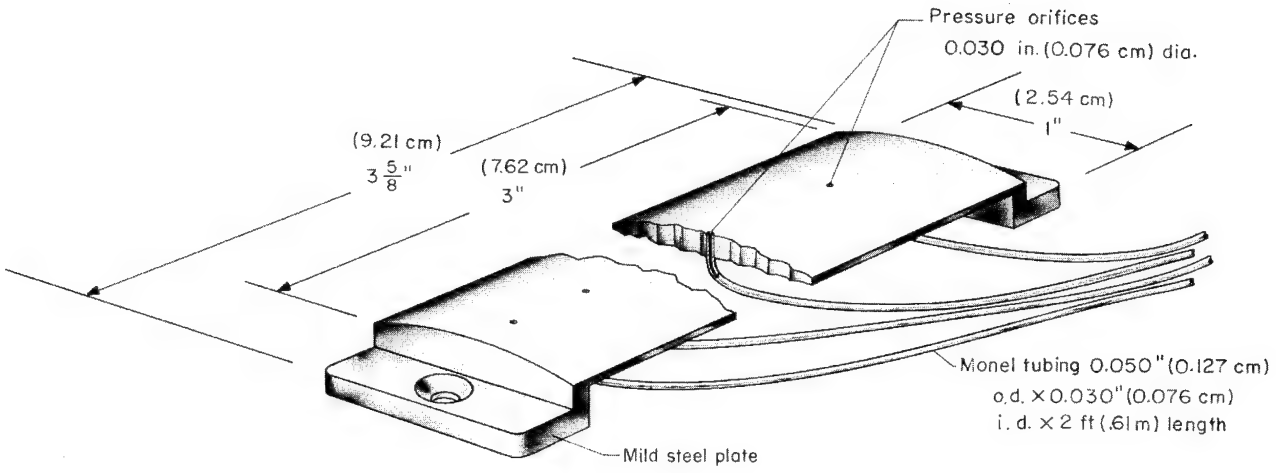

Figure 5.- Pressure-distribution model.

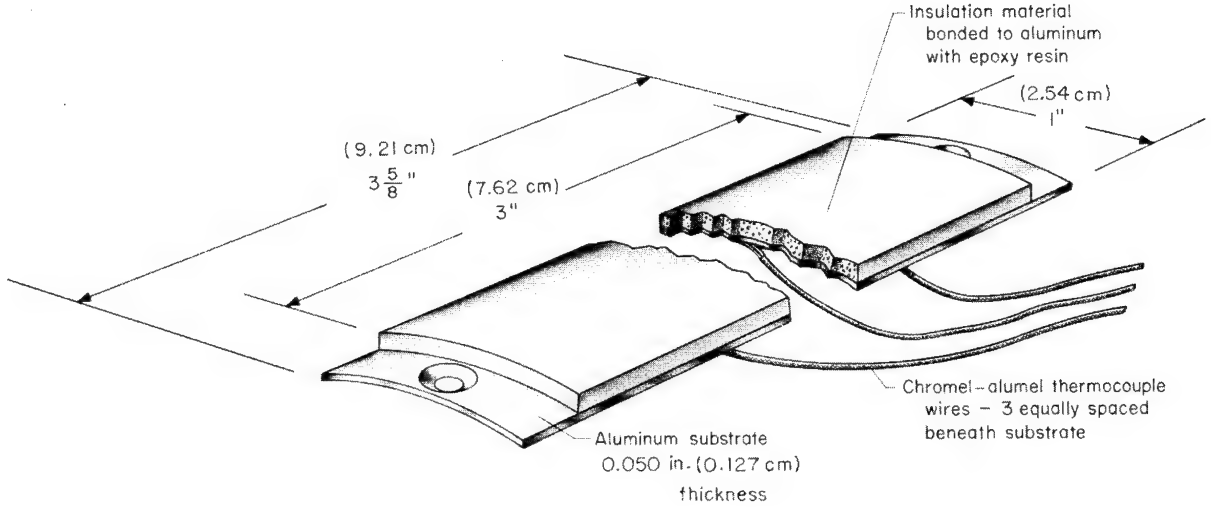

Figure 6.- Model of material test specimen.

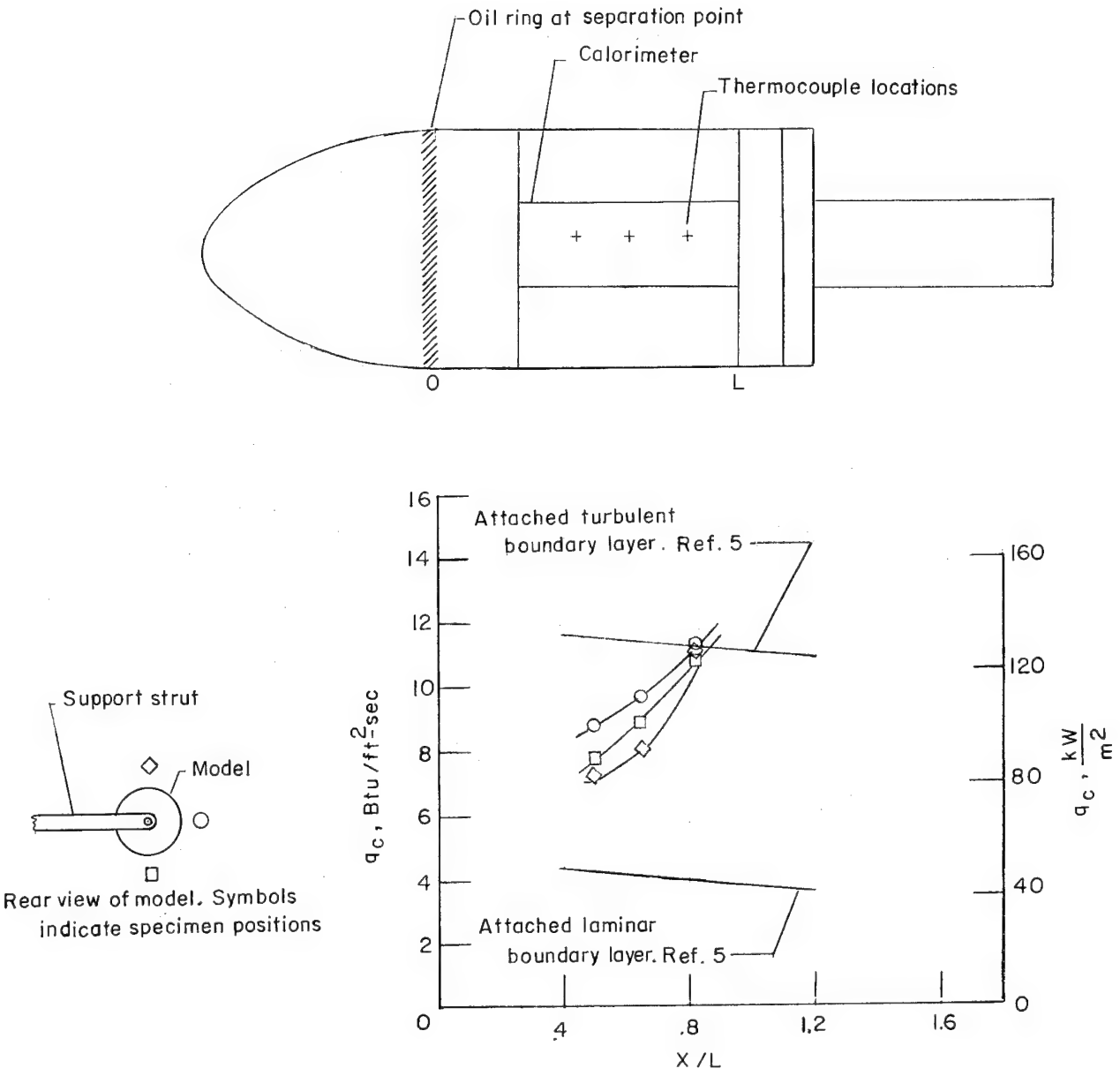

Figure 7.- Heat-transfer distribution over specimen positions.

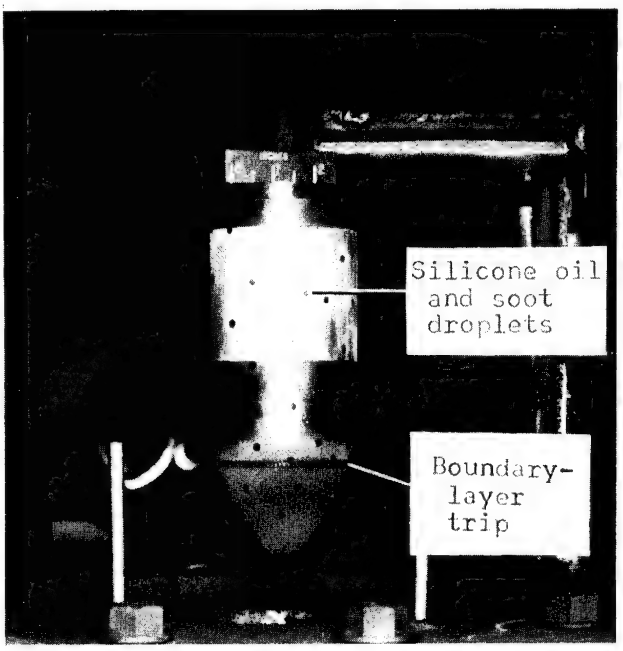

(a) Before test. L-64-5682.1

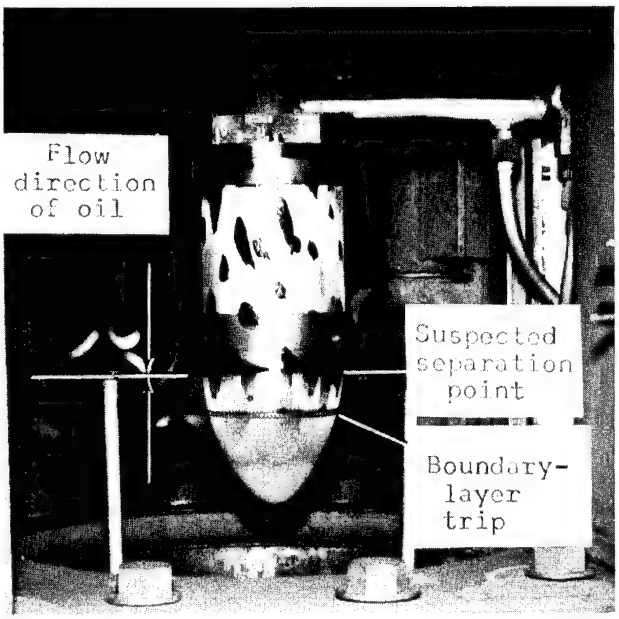

(b) After test. L-64-5683.1

Figure 8.- Oil flow on surface of rounded ogive nose and cylindrical body during typical test.

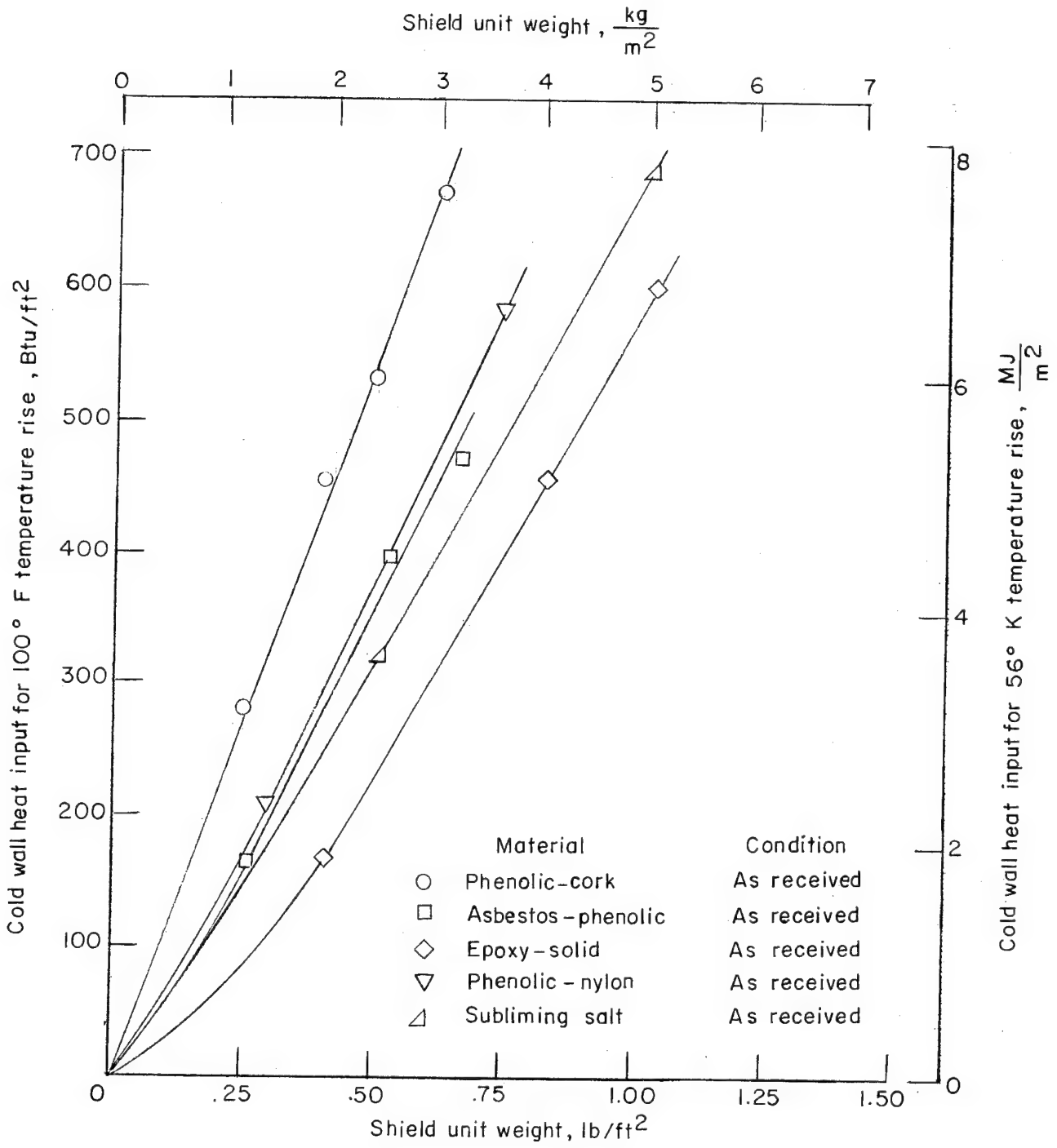

Figure 9.- Comparison of materials on the basis of the cold wall heat input required for a 100° F (56° K) temperature rise.

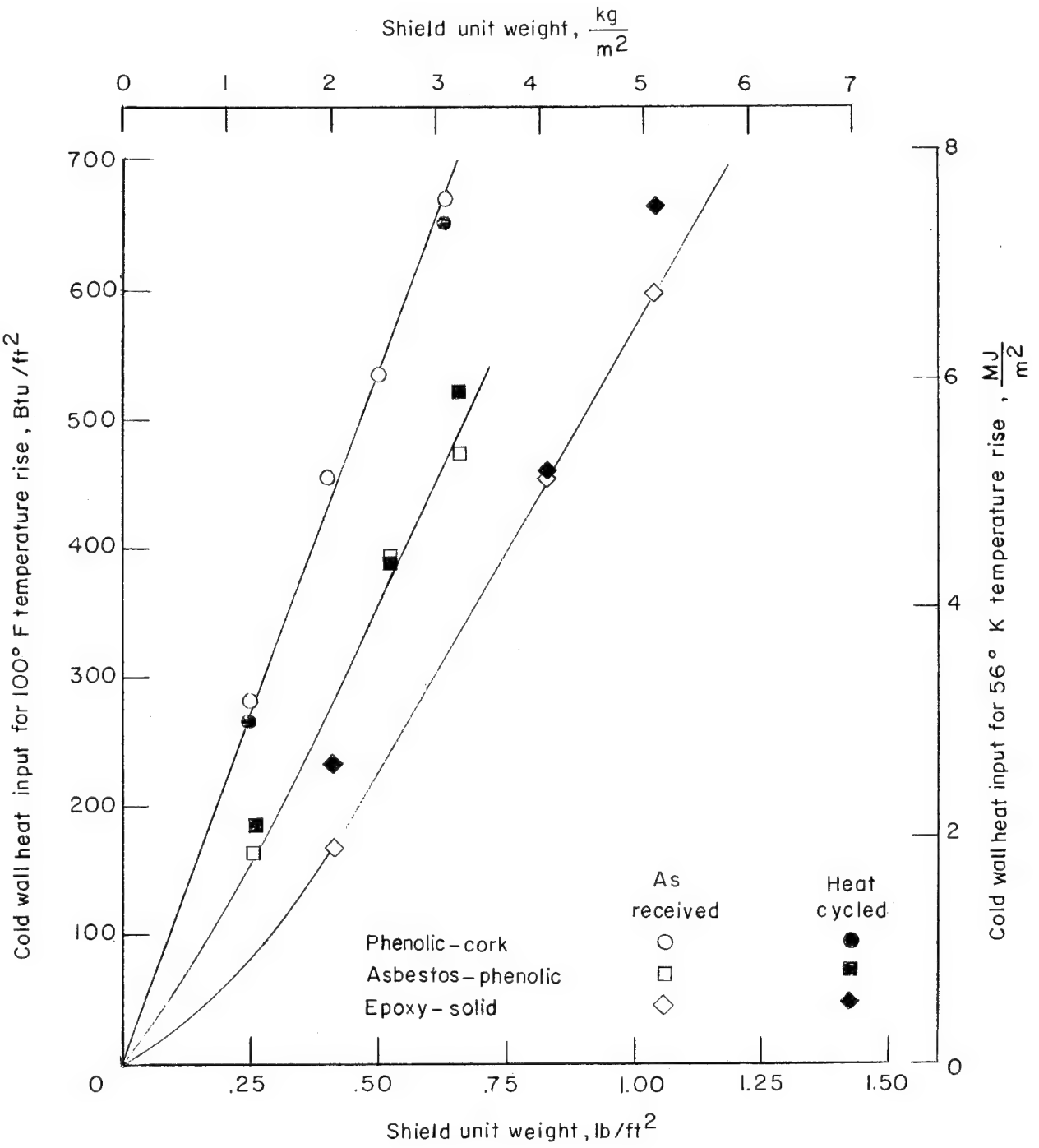

Figure 10.- Comparison of heat cycled specimens with specimens tested as received from the manufacturer.

Rear of specimens Specimen profile before testing Front of specimens

(a) Phenolic-cork composition.

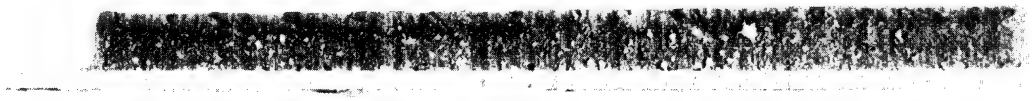

(b) Asbestos-phenolic composition.

(c) Subliming-salt composition.

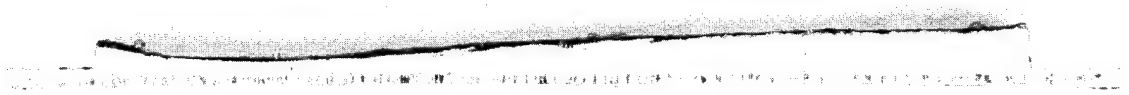

(d) Epoxy-solid composition.

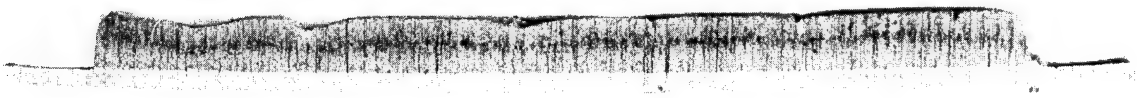

(e) Phenolic-nylon composition.

Figure 11.- Sectioned specimens after testing. L-65-189

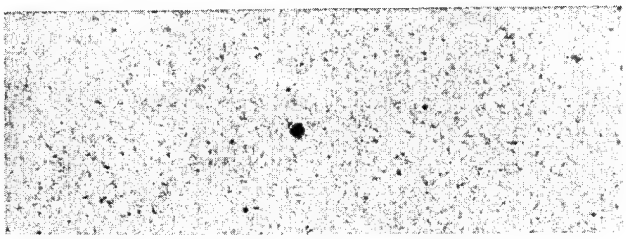

Before test

Front of specimens After test Rear of specimens

(a) Phenolic-cork composition.

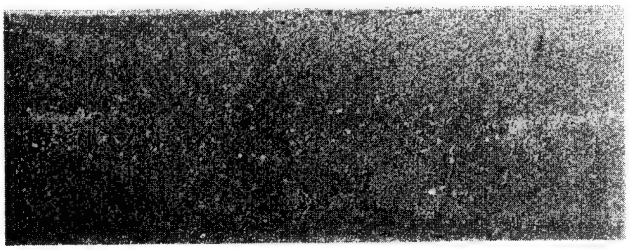

Before test

After test

(b) Phenolic-nylon, PN-4.

Figure 12.- Surface of specimens before and after testing. L-65-190

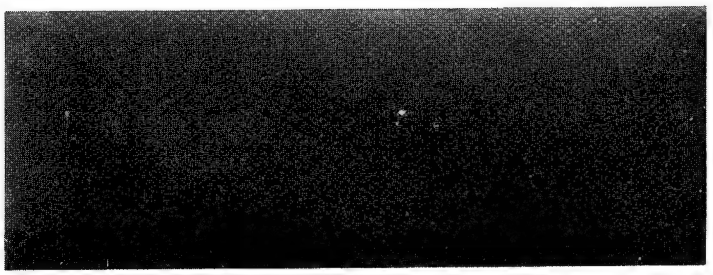

Before test

Front of specimens After test Rear of specimens

(c) Subliming-salt composition.

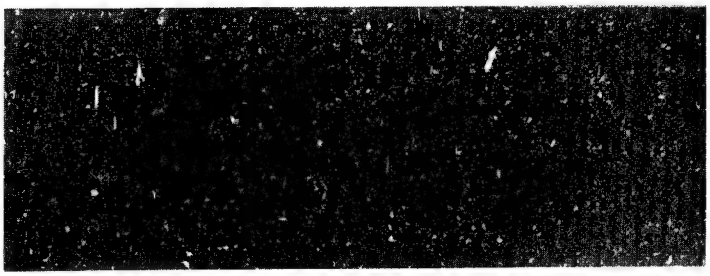

Before test

After test

(d) Asbestos-phenolic composition. L-65-191

Figure 12.- Continued.

Before test

Front of specimens

Rear of specimens

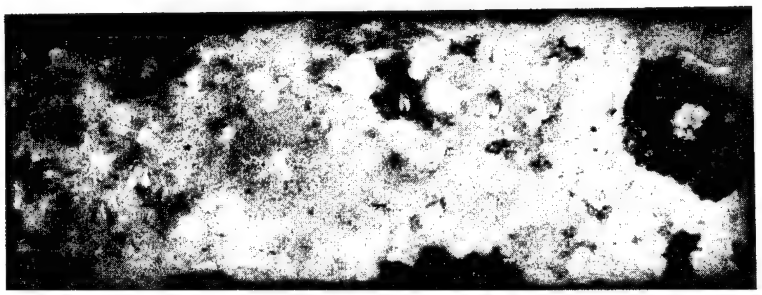

After test

(e) Epoxy-solid composition. L-65-192

Figure 12.- Concluded.

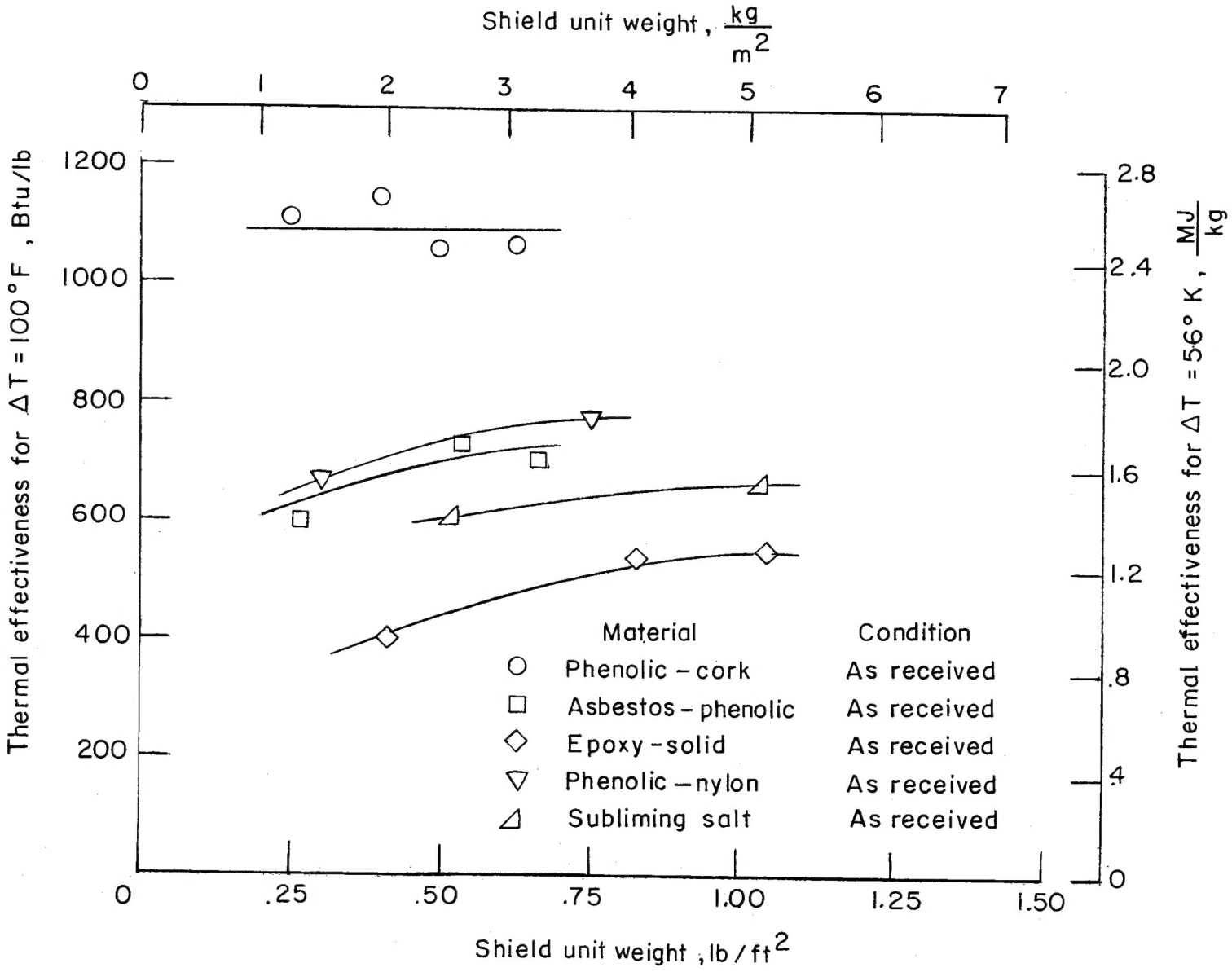

Figure 13.- Variation of thermal effectiveness with shield unit weight.

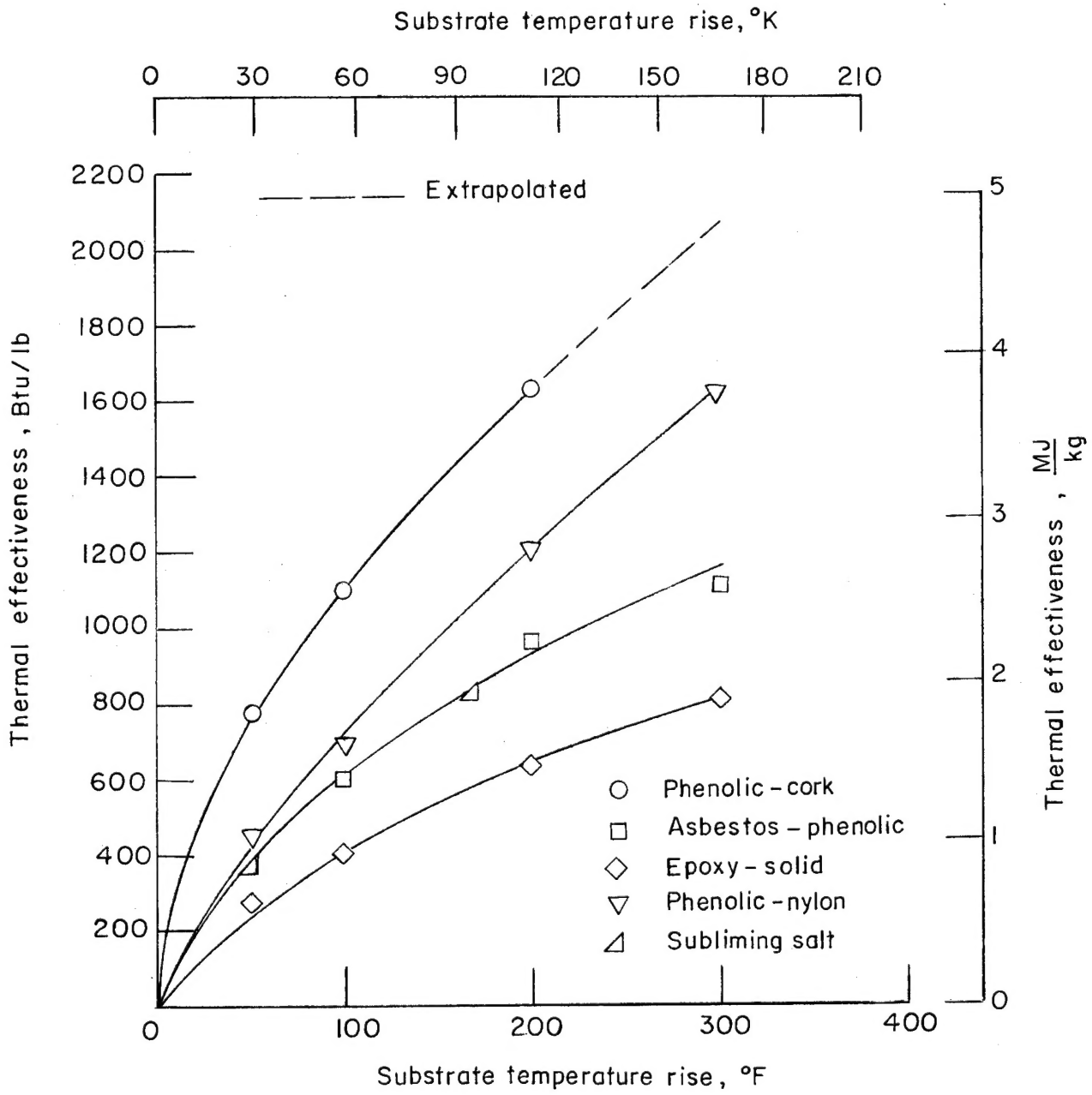

Figure 14.- Thermal effectiveness as a function of substrate temperature rise for 0.1-inch-thick (2.54-cm) specimens as received from the manufacturer.

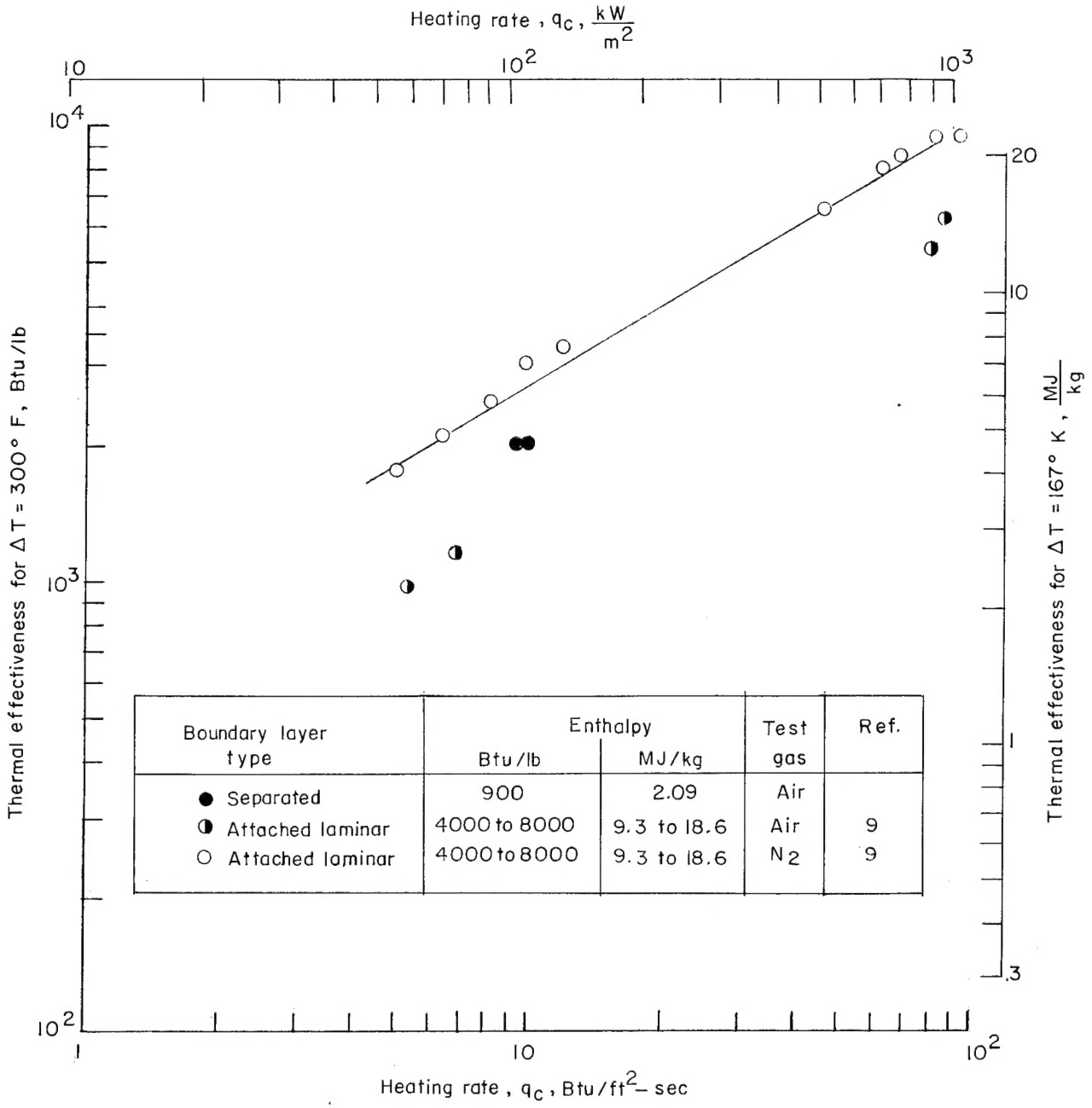

Boundary layer type	Enthalpy Btu/lb	Enthalpy MJ/kg	Test gas	Ref.
● Separated	900	2.09	Air	
◑ Attached laminar	4000 to 8000	9.3 to 18.6	Air	9
○ Attached laminar	4000 to 8000	9.3 to 18.6	N_2	9

Figure 15.- Comparison of phenolic-cork thermal effectiveness in a separated and attached boundary layer.

NASA-Langley, 1965 L-4554

"The aeronautical and space activities of the United States shall be conducted so as to contribute . . . to the expansion of human knowledge of phenomena in the atmosphere and space. The Administration shall provide for the widest practicable and appropriate dissemination of information concerning its activities and the results thereof."

—NATIONAL AERONAUTICS AND SPACE ACT OF 1958

NASA SCIENTIFIC AND TECHNICAL PUBLICATIONS

TECHNICAL REPORTS: Scientific and technical information considered important, complete, and a lasting contribution to existing knowledge.

TECHNICAL NOTES: Information less broad in scope but nevertheless of importance as a contribution to existing knowledge.

TECHNICAL MEMORANDUMS: Information receiving limited distribution because of preliminary data, security classification, or other reasons.

CONTRACTOR REPORTS: Technical information generated in connection with a NASA contract or grant and released under NASA auspices.

TECHNICAL TRANSLATIONS: Information published in a foreign language considered to merit NASA distribution in English.

TECHNICAL REPRINTS: Information derived from NASA activities and initially published in the form of journal articles.

SPECIAL PUBLICATIONS: Information derived from or of value to NASA activities but not necessarily reporting the results of individual NASA-programmed scientific efforts. Publications include conference proceedings, monographs, data compilations, handbooks, sourcebooks, and special bibliographies.

Details on the availability of these publications may be obtained from:

SCIENTIFIC AND TECHNICAL INFORMATION DIVISION

NATIONAL AERONAUTICS AND SPACE ADMINISTRATION

Washington, D.C. 20546